Control of pH and Its Effect on Electrochemical Behavior and Corrosion Product Release of Materials in PWR Primary Water Chemistry System

Hee Kwon Ku[a*], Jae Seon Cho[a], Chang Kyu Chung[b], One Yoo[b], Jong Soo Kim[b]
[a]*FNC Technology, 13 Heungdeok 1-ro, Yongin-si, Gyeonggi-do, 16954, Korea*
[b]*KEPCO E&C, 269 Hyeoksin-ro, Gimcheon-si, Gyeongsangbuk-do, 39660, Korea,*
**Corresponding author: ku@fnctech.com*

1. Introduction

An integral type of pressurized water reactor (PWR), called System integrated Modular Advanced ReacTor (SMART) is being developed in Korea, mainly by a team of KEPCO and KAERI. This small size unit is designed for electricity generation as well as thermal applications, such as seawater desalination, for meeting the economic advantage and reliable safety requirement [1-3]. Materials used in SMART system are similar ones used in conventional PWR, e.g., Zr alloy cladding, low alloy steel, stainless steel, and Ni alloys [3].

Water chemistry condition to be considered in SMART system is also based on current typical PWR water chemistry, but without H_3BO_3. The major reason to eliminate H_3BO_3 is to avoid an axial offset anomaly (AOA) and related corrosion concerns and consequently minimizes various Chemical &Volume Control System (CVCS). This greatly results in reduction operating cost and volume of chemical wastes. In addition, use of KOH to control pH is proposed [4].

Nevertheless, electrochemical corrosion behavior of critical component materials has not been studied systematically under various pH ranges controlled singly by KOH without addition of H_3BO_3. Thus, the purpose of this study was to evaluate the corrosion characteristics of major alloys in SMART system at different pHs without H_3BO_3 in 340°C water containing various concentrations of KOH.

2. Experimental Procedures

2.1. Water Chemistry Control

A high pressure, high temperature water loop has been assembled to simulate the PWR primary side water chemistry. An optimum water chemistry condition, such as pH, KOH or LiOH with and without H_3BO_3, and 25cc/kg of H_2 was maintained during the course of test duration. An Ar gas was purged to remove the dissolve O_2 or air and pH of water adjusted by LiOH or KOH. All tests were conducted at 340°C and 2500psi in a recirculating water loop. Table I shows the test water chemistry condition.

Table I: Test Water Chemistry Condition

Comments	With H_3BO_3	Without H_3BO_3
pH Control	LiOH	KOH
Temperature(℃)	340℃	340℃
Pressure(psi)	2500psi	2500psi
H_2 gas(25℃)	25cc/kg H_2O	25cc/kg H_2O
pH_T	7, 8, 9, 10	7, 8, 9, 10
Coolant Water	1600ppm H_3BO_3	-

Fig. 1 shows the schematic drawing for the water sampling line directly from the high temperature water. A water sample was collected every day for 15 days directly from the high temperature test water after exposing to a given water chemistry. All water specimens were analyzed by an Atomic Absorption (AA)-graphite or an inductively coupled plasma-mass spectrometry (ICP-MS).

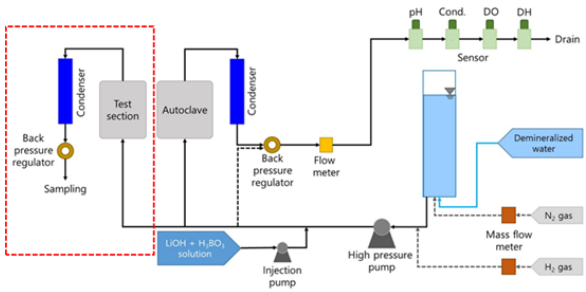

Fig. 1. Schematic of test loop for the water sampling line in high pressure, high temperature water

2.2. Preparation & Analysis of Test Specimens & Water

A small coupon shape (1cm x 1cm x 0.4cm) of test specimens (ZIRLO, SA508, SS304, Alloy 690) was polished by a SiC paer 200 and arranged in a SS sample hanger and immersed in an 1 gallon SS316L autoclave. Table II lists the composition of test alloy. Specimens for measuring the electrochemical corrosion behavior was spot-welded using an Teflon insulated SS wire, mounted in a Conax fitting for an electrical connection and was analyzed by using a Gamry Instrument (Gamry Reference 600 Potentiostat). A Cu/Cu_2O pH electrode was used as a reference electrode and a piece of Pt flag as a counter electrode. All specimens and electrodes were installed in a 1 gallon 316S SS autoclave.

After immersion for 3 days, electrochemical corrosion test and analysis was performed by ASTM G59 and ASTM G102-89. Both ASTM articles describe the method for calculating of corrosion rate using electrochemical parameters from the electrochemical polarization behaviors of each alloy. The nature of oxide formed on each specimen was analyzed by a x-ray photoelectron spectroscopy (XPS) and a scanning electron microscopy (SEM).

Table II: Composition of Test Alloys

	C	Mn	P	S	Si	Cr	Ni	Mo	V	Cu	Al	Fe
Stainless steel 304	0.03	2	0.045	0.03	1	18.11	9.1	-	-	-	-	-
SA-508 Grade 3 Class 1	0.2	1.35	0.007	0.001	0.22	0.2	0.91	0.51	0.004	0.02	0.02	-
Alloy 690	0.03	0.18	-	0.015	0.03	29.4	-	-	-	0.01	-	10
	Nb	Sn	Fe	Cr	Ni	O						
ZIRLO	0.9	0.9	0.1	-	-	0.11						

3. Experimental Results and Discussion

3.1.Measurement of Corrosion Rate and Oxide Analysis

3.1.1. Corrosion Characteristic of 304 SS

Corrosion behavior of 304 SS was examined in 340C water containing 25cc/kg H_2 and LiOH+1600ppm H_3BO_3 or KOH at various pHs of 7 (no KOH addition), 8, 9, and 10. As shown in Fig. 5, corrosion rates of 304 SS are estimated to be about 0.5mil/year, regardless the H_3BO_3 presence and pH. It is shown that chemical agent for controlling the pH of water and relevant pH did not alter the corrosion behavior of 304 SS. As shown in Figures 6 and 7, this evidence was clearly supported by the oxide analysis by SEM and XPS, indicating the similar oxide natures such as the oxide thickness (~25nm) and chemistry. The crystalline shape of oxide particulates at the outer oxide surface is predominant. XPS result also clearly indicates the presence of a duplex oxide film, consisting of a Fe rich outer layer and a Cr-enriched inner oxide layer (e.g., $FeCr_2O_4$). One can thus state that the presence of H_3BO_3 did not affect the corrosion behavior of 304 SS either in LiOH or in KOH environment.

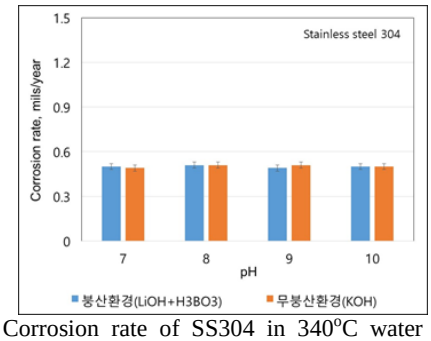

Fig. 5. Corrosion rate of SS304 in 340°C water with and without H_3BO_3

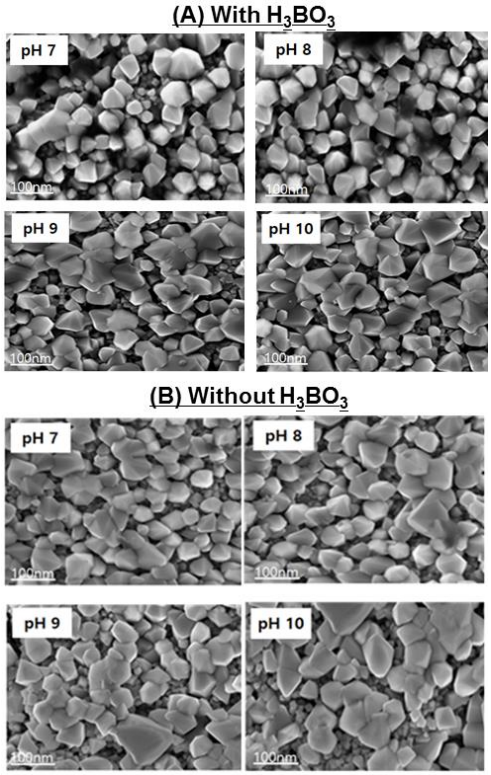

Fig. 6. Surface morphology of oxide formed on SS304 in 340°C water (A) with and (B) without H_3BO_3.

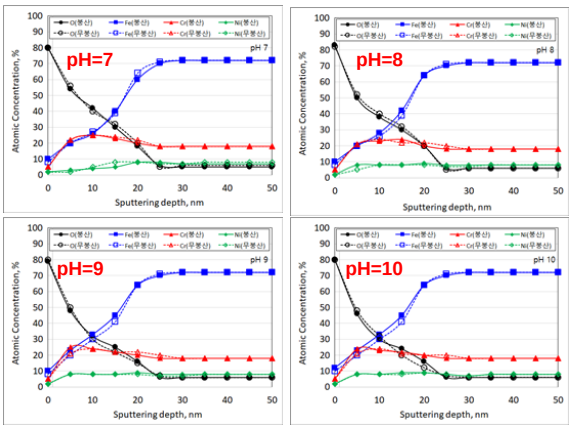

Fig. 7: XPS analysis of oxide formed on SS304 in 340°C water at various pHs with and without H_3BO_3.

3.1.2. Corrosion Characteristic of SA-508 Alloy

Corrosion behavior of SA-508 alloy was examined in 340C water containing 25cc/kg H_2 and LiOH+1600ppm H_3BO_3 or KOH at various pHs of 7 (no KOH addition), 8, 9, and 10. As shown in Fig. 8, corrosion rates of SA-508 are estimated to be about 1.1mil/year, regardless the H_3BO_3 presence and pH. As shown in Fig. 9, this evidence was also clearly supported by the oxide analysis by SEM. The similar but larger crystalline shape of oxide particulates, compared to ones on 304 is clearly evident. XPS result shows relatively higher in Cr concentration at the oxide/matrix interface with the similar oxide thickness (~25nm).. Thus, so significant

effect of H_3BO_3 on the corrosion behavior of SA-508 alloy either in LiOH or in KOH environment was measured.

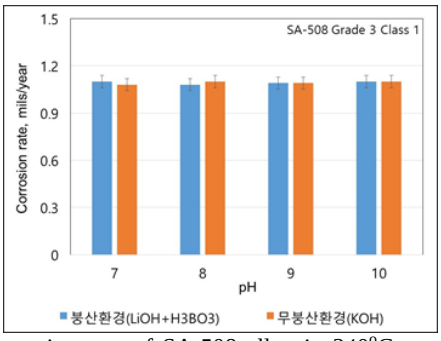

Fig. 8. Corrosion rate of SA-508 alloy in 340°C water with and without H_3BO_3.

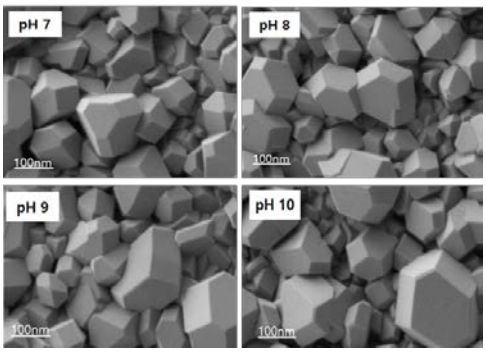

Fig. 9. Surface morphology of oxide formed on SA-508 alloy in 340°C water with H_3BO_3.

3.1.3. Corrosion Characteristic of Alloy 690

Electrochemical corrosion behavior of Alloy 690 was examined in 340oC water containing 25cc/kg H_2 and LiOH+1600ppm H_3BO_3 or KOH at various pHs of 7 (no KOH addition), 8, 9, and 10. As shown in Figure 10, corrosion rates of Alloy 690 are estimated to be about 0.3mil/year, regardless the H_3BO_3 presence and pH. This corrosion rate of Alloy 690 is little lower than one of 304 SS. Fig. 11 shows the oxide surface morphology analyzed by SEM, indicating the similar oxide natures and a smaller crystalline shape of oxide particulates, compared to ones on 304 is clearly evident. XPS result shows the similar chemistry at the similar oxide thickness (~20nm) and relatively higher in Ni and Cr concentration at the oxide/matrix interface, a possible indication of Ni/Cr spinel oxide formation. Thus, once can assume that the presence of Ni/Cr spinel (e.g., $NiCr_2O_4$) protects against the dissolution of matrix so that no significant effect of H_3BO_3 expects on the corrosion behavior of SA 508 alloy either in LiOH or in KOH environment was measured.

3.1.4. Corrosion Characteristic of ZIRLO

Corrosion behavior of ZIRLO was examined in 340°C water containing 25cc/kg H_2 and LiOH+1600ppm H_3BO_3 or KOH at various pHs of 7 (no KOH addition), 8, 9, and 10.

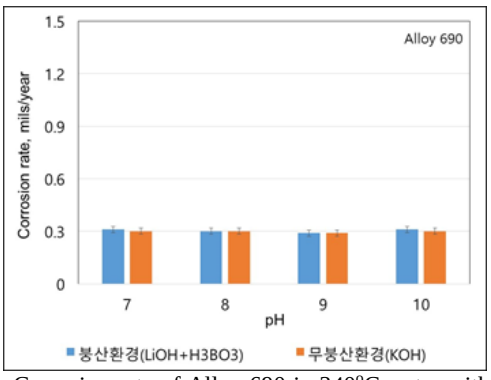

Fig. 10. Corrosion rate of Alloy 690 in 340°C water with and without H_3BO_3.

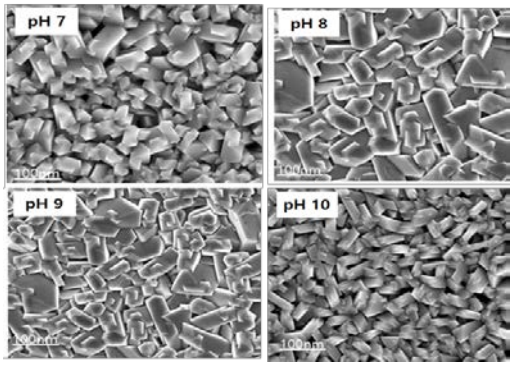

Fig. 11. Surface morphology of oxide formed on Alloy 690 in 340°C water with H_3BO_3.

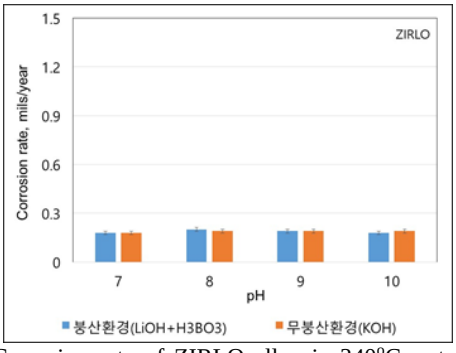

Fig.12. Corrosion rate of ZIRLO alloy in 340°C water with and without H_3BO_3.

As shown in Fig. 12, the corrosion rate of ZIRLO was estimated to be about 0.2mil/year, regardless the H_3BO_3 presence and pH. The oxide surface morphology analyzed by SEM, indicating the similar oxide natures and. XPS result also confirms the similar chemistry at the similar oxide thickness (5nm) and the presence of Zr and O signal, indicating a ZrO_2 layer that is well known as a protective oxide. Due to a low resolution sensitivity of XPS, B normally observed on Zr oxide, was not detected through the thickness of Zr oxide. Thus, once can assume that the presence of a thin/dense Zr oxide provide a protectiveness on ZIRLO that

eventually hinders the corrosion behavior of ZIRLO either in LiOH or in KOH environment with and without addition of H_3BO_3..

3.2.Measurement of Corrosion Product Release Rate

The release of corrosion products to the coolant water can be related to conditions, such as pH and chemistry, that eventually influence the formation of the oxide layer. The water flow dynamic also expects to play a critical role that removes the soluble ions before they have a chance to precipitate back on the oxide layer. Thus, it is very important to understand the release and transport of both particulates and soluble ions in a coolant.

The corrosion product release test of 304 SS and SA 508 alloy, respectively, after exposing for given period of immersion time to 340°C water containing 25cc/kg H_2 at 2500psi. The pH of water was controlled by addition of LiOH+1600ppm H_3BO_3 or KOH only to be ~7. In absence of H_3BO_3, additional [K^+] at 100ppm was adjusted by adding a proper amount of potassium oxalate monohydrate, $(COOK)_2H_2O$.

Fig. 13 shows the corrosion product release rate as a function of immersion time of 304SS with and without addition of H_3BO_3. Regardless the presence or absence of H_3BO_3, major ionic species were Fe and Ni and it is also clearly evident that both Fe and Ni containing corrosion products were increased for a few days and stabilized afterward. This can be explained by the formation of Cr-enriched spinel oxide in an inner oxide layer adjacent to the substrate. It is well documented that the Cr-rich spinel oxide layer prevents the dissolution of SS matrix. Previous XPS analysis confirms the presence of Cr enrichment in an inner oxide layer (Fig. 7).

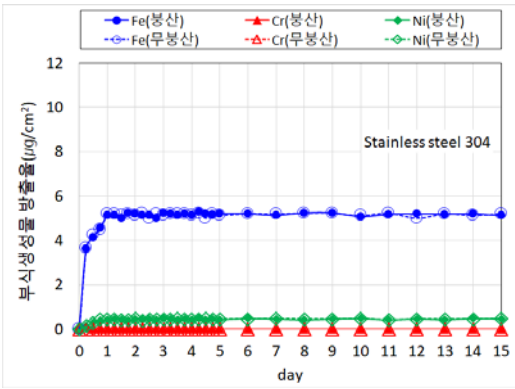

Fig. 13. Corrosion product release rate from 304 SS in 340°C water with and without H_3BO_3.

Fig. 14 shows the corrosion product release as a function of immersion time of SA 508 alloy with and without addition of H_3BO_3. Regardless the presence or absence of H_3BO_3, major ionic species was Fe, and it is also clearly evident that a Fe containing corrosion products were increased for a few days and stabilized afterward. This is very similar behavior as one on 304SS. This can be mainly due to the formation of a thick Fe oxide as confirmed on Fig. 9.

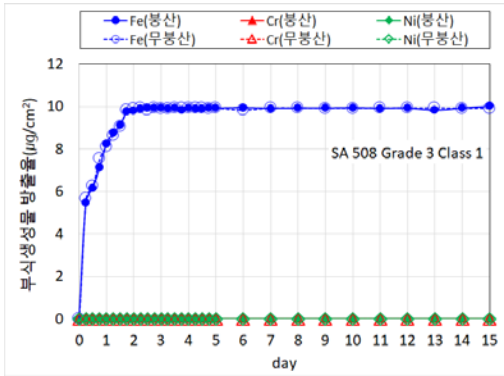

Fig. 14. Corrosion product release rate from SA-508 alloy in 340°C water with and without H_3BO_3.

4. Summary

Corrosion behavior and corrosion product release rate of various alloys (SS304, SA-508 alloy, Alloy 690 and ZIRLO), were investigated in 340°C water at various ranges of pHs (7-10), containing LiOH or KOH solution with and with addition of H_3BO_3. Laboratory results show that the general corrosion behavior and the microstructure and chemistry of oxide layers formed on test alloys were not significantly affected by various pHs and the presence of H_3BO_3. Furthermore, there was no significant effect of water chemistry on the corrosion product release rate from all test alloys. Thus, based on short term laboratory data, one can conclude that the reliability and safety of primary materials in SMART system can be maintained in 340°C water containing only KOH even without addition of H_3BO_3.

Acknowledgement

This work was performed under a contract with KEPCO E&C Company (Contract No: C0091720049).

References

[1]표준설계부,“ SMAR 개발사업단” , 한국원자력연구원
[2] H-C Kim, Y-J Chung, K-H Bae, and S-Q Zee, “Safety Analysis of SMART”, GENES4/ANP2003, Sep. 15-19, 2003, Kyoto, Japan.
[3] “Evaluation of Corrosion Characteristics of SMART Materials (III), KAERI/CR-234/2005
[4] Keith Fruzzetti, “Potassium Hydroxide for LWR Primary Coolant pH Control Feasibility Assessment”, International Light Water Reactor Materials Reliability Conference and Exhibition, 2016